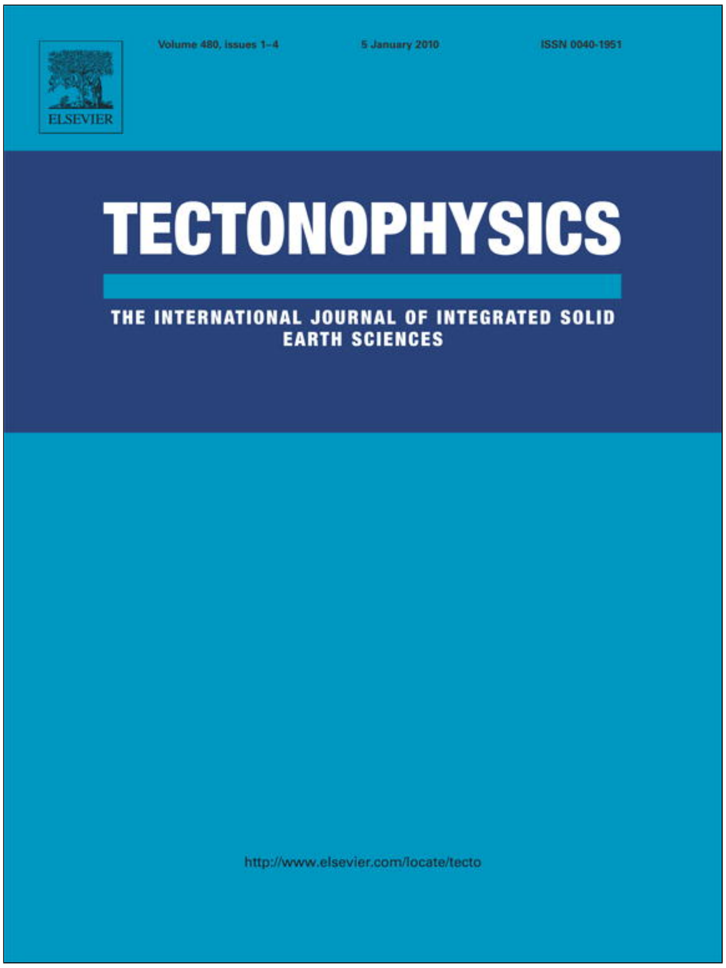
Volume 480, issues 1–4
5 January 2010
ISSN 0040-1951
ELSEVIER
TECTONOPHYSICS
THE INTERNATIONAL JOURNAL OF INTEGRATED SOLID EARTH SCIENCES
http://www.elsevier.com/locate/tecto

Tectonophysics 480 (2010) 48–56

Contents lists available at ScienceDirect

Tectonophysics

journal homepage: www.elsevier.com/locate/tecto

The intracratonic Caraíbas–Itacarambi earthquake of December 09, 2007 (4.9 m_b), Minas Gerais State, Brazil

Cristiano Chimpliganond [a,*], Marcelo Assumpção [b], Mônica Von Huelsen [a], George Sand França [a]

[a] Seismological Observatory, University of Brasilia, Brasilia, 70910-000, Brazil
[b] Institute of Astronomy, Geophysics and Atmospheric Sciences, University of São Paulo, 05508-090, São Paulo, Brazil

ARTICLE INFO

Article history:
Received 25 March 2009
Received in revised form 15 September 2009
Accepted 16 September 2009
Available online 26 September 2009

Keywords:
Intracratonic earthquake
Intraplate seismicity
Focal mechanism
São Francisco Craton
Brazilian seismicity

ABSTRACT

On December 9, 2007, a 4.9 m_b earthquake occurred in the middle of the São Francisco Craton, in a region with no known previous activity larger than 4 m_b. This event reached intensity VII MM (Modified Mercalli) causing the first fatal victim in Brazil. The activity had started in May 25, 2007 with a 3.5 magnitude event and continued for several months, motivating the deployment of a local 6-station network. A three week seismic quiescence was observed before the mainshock. Initial absolute hypocenters were calculated with best fitting velocity models and then relative locations were determined with hypoDD. The aftershock distribution indicates a 3 km long rupture for the mainshock. The fault plane solution, based on P-wave polarities and hypocentral trend, indicates a reverse faulting mechanism on a N30°E striking plane dipping about 40° to the SE. The rupture depth extends from about 0.3 to 1.2 km only. Despite the shallow depth of the mainshock, no surface feature could be correlated with the fault plane. Aeromagnetic data in the epicentral area show short-wavelength lineaments trending NNE–SSW to NE–SW which we interpret as faults and fractures in the craton basement beneath the surface limestone layer. We propose that the Caraíbas–Itacarambi seismicity is probably associated with reactivation of these basement fractures and faults under the present E–W compressional stress field in this region of the South American Plate.

1. Introduction

The mid-plate region of the South American Plate is characterized by very low rate of seismicity, typical of stable continental interior. The seismicity in Brazil shows maximum magnitude of 6.2 m_b (Barros et al., 2009) which is lower than the maximum observed in other intraplate regions, such as Eastern North America, Australia and India where magnitudes larger than 7 have occurred (Johnston, 1989; Johnston and Kanter, 1990; Johnston, 1996; Schulte and Mooney, 2005). Despite the low magnitudes in Brazil, maximum intensities of VII MM (Modified Mercalli) are relatively common (e.g., Berrocal et al., 1984; Ferreira et al., 1998) making seismic risk evaluation an important issue in projects of critical facilities such as nuclear installations. On December 9, 2007, a 4.9 m_b earthquake occurred in the middle of the São Francisco Craton (Fig. 1). This event with epicenter near Itacarambi city, State of Minas Gerais, caused the first fatal victim in Brazil, injured six persons, damaged 76 buildings, reaching intensity VII MM in the Caraíbas village. All the inhabitants of Caraíbas were displaced to new houses constructed by the Minas Gerais State government at Itacarambi city, located about 36 km east. At Caraíbas, on May 24, 2007, occurred a 3.5 magnitude event. According to historical records of the last century or more this was the first earthquake ever reported at an area with radius of 30 km from Caraíbas village (Berrocal et al., 1984).

The models proposed to explain the intraplate seismicity consider that the earthquakes result from ruptures in weakness zones or from stress concentration (e.g. Sykes, 1978; Talwani, 1989; Talwani and Rajendran, 1991; Kenner and Segal, 2000). Correlations between crustal zones of weakness, such as extended crust in aborted rifts or continental margins, and intraplate earthquakes have been made (Johnston, 1989; Schulte and Mooney, 2005). Stress concentration in the upper crust due to structural inhomogeneities is also used to try to explain intraplate seismicity (Sykes, 1978; Talwani, 1989; Talwani and Rajendran, 1991; Kenner and Segal, 2000; Assumpção et al., 2004).

About half of the earthquakes larger than 5.0 m_b in Brazil have occurred near the continental margin (Assumpção, 1998; Barros et al., 2009) which is a common feature of intraplate seismicity (Johnston and Kanter, 1990; Schulte and Mooney, 2005). Of the remaining epicenters in the continental interior, nine are located at the border or inside Phanerozoic basins and one lies in a Neoproterozoic/Paleozoic fold belt. On the other hand, no major structural feature is known in the middle of the São Francisco Craton that could be easily associated with the 2007 event. The study of the 2007 earthquake, therefore, is important to help understand the causes of mid-plate seismicity in stable continental interiors.

* Corresponding author. Fax: +55 61 32745927.
E-mail addresses: naibert@unb.br (C. Chimpliganond), marcelo@iag.usp.br (M. Assumpção), monisis@unb.br (M. Von Huelsen), georgesand@unb.br (G.S. França).

0040-1951/$ – see front matter © 2009 Elsevier B.V. All rights reserved.
doi:10.1016/j.tecto.2009.09.016

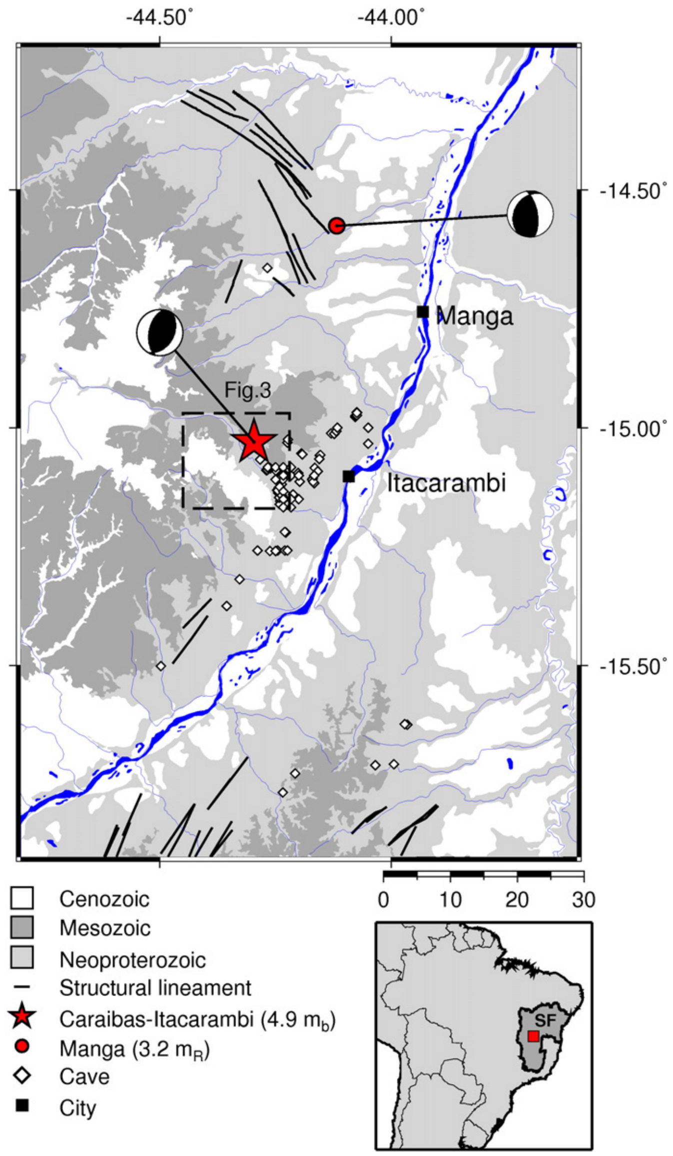

Fig. 1. Geologic map of the Caraíbas–Itacarambi/MG area (CPRM, 2003). The red star and the red circle indicate the epicentral locations of the Caraíbas–Itacarambi earthquake of December 9, 2007 (4.3 m_R) (this work) and the Manga earthquake of March 1st, 1990 (3.2 m_R) (Assumpção et al., 1990) with the focal mechanisms (beach balls). The structural lineaments are from CPRM (2003) and the open diamonds correspond to mapped caves (CECAV, 2007). The dashed square corresponds to the area of Fig. 3. In the bottom right the map shows the geographic location of the study area (red square).

In this paper we present the results obtained with a local seismographic network installed in the area of the Caraíbas village forty six days before the mainshock occurrence. The data set comprises foreshocks, the mainshock and aftershocks, including also two large aftershocks with magnitudes of 3.8 m_b and 3.1 m_D. The equipments and the financial support used in the field campaigns to deployment of the seismic network and the macroseismic survey were given by the Seismological Observatory of the University of Brasília (SIS/UnB).

2. Geological setting

The stable South American Platform is composed mainly of Precambrian cratonic blocks, the largest being the Amazonian Craton, in the north, and the São Francisco Craton, in the east. Between these cratonic masses mobile belts were created and deformed during Neoproterozoic times (Tassinari et al., 2000).

The epicentral area of Caraíbas–Itacarambi is located in the middle of the São Francisco Craton (Fig. 1). Its evolution started in the Archean and ended at the close of the Mesoproterozoic. The São Francisco Craton is part of the Gondwana Neoproterozoic supercontinent, formed by agglutination of continental masses which were involved in multiple and successive collisions (Cordani et al., 2000). The basement of the São Francisco Craton comprises medium to high-grade metamorphic terranes of Archean age, mainly gneiss and granitic rocks, of the Januária Complex (Nobre-Lopes, 2002; CPRM, 2003; Martínez, 2007). These rocks were last deformed/metamorphosed before 1.8 Ga. During Neoproterozoic times, a sequence of platform to continental sedimentary rocks (Bambuí Group) was deposited over the cratonic basement. This group is represented in the study area by limestones, dolomites and siltstones, with minor presence of marbles (Nobre-Lopes, 2002; Martínez, 2007). The predominance of limestones and dolomites of the Sete Lagoas Formation (Bambuí Group) in the area can be observed in Fig. 1 by the several caves (open diamonds) mapped mainly between the village of Caraíbas and the city of Itacarambi (CECAV, 2007). This karstic domain is also indicated by the discontinuation of the Peruaçu River, as can be seen in Fig. 3. Nevertheless, the tectonic origin for the Caraíbas–Itacarambi seismicity can be proved as will be seen in the next sections. Overlying these units are Mesozoic eolic sandstones of the Urucuia Group and alluvium and detritic–lateritic covers of Cenozoic age. Structural lineaments mapped to the south of Caraíbas show NE–SW trend, being rotated anti-clockwise to the north to NW–SE (CPRM, 2003; Nobre-Lopes, 2002; Martínez, 2007) as shown in Fig. 1. The focal mechanism obtained by Assumpção et al. (1990) for a 3.2 m_R earthquake occurred on March 1st, 1990, about 20 km to the NW of Manga city also suggest an anti-clockwise rotation in respect to the focal mechanism obtained for the Caraíbas–Itacarambi seismicity (this work).

3. Seismological data

3.1. The mainshock of December 9, 2007

Small earthquakes started to occur in the village of Caraíbas, north of Minas Gerais State, on May 24, 2007, when a 3.5 magnitude event produced some cracks in poor quality houses, constructed some years ago, consisting of adobe masonry and with walls built up using earth bricks unconnected to wooden beams and columns.

The mainshock of December 9, 2007 (4.9 m_b) produced intense damage in the village of Caraíbas, mainly in these adobe houses. The maximum intensity reached VII MM (red area in Fig. 2), producing the first fatal victim of an earthquake ever reported in Brazil. The best constructed houses, with reinforced concrete frame structures and masonry infill, suffered only few superficial wall cracks. This mainshock was felt up to 80 km away from Caraíbas, and the isoseismal of VI MM intensity comprise an area of about 100 km^2. Fig. 2 shows the isoseismal map for the Caraíbas–Itacarambi mainshock with the isoseismal curves (dashed lines). The symbols correspond to Modified Mercalli intensity values obtained at the places where macroseismic questionnaires were applied to the citizens during the first weeks after the mainshock occurrence.

Table 1 shows the source parameters for the December 9, 2007 earthquake determined by the International Data Center (IDC), National Earthquake Information Center (NEIC/USGS) and this paper. The epicenters are shown in Fig. 3. Magnitudes were also calculated using data from six stations in the range 200 to 1500 km distance, using the regional magnitude scale for Brazil m_R (Assumpção 1983), based on the maximum particle velocity of the P-wave train, which is equivalent to the teleseismic m_b scale. The regional magnitude of the mainshock is $m_R = 4.3$, lower than the teleseismic 4.9 m_b (NEIC).

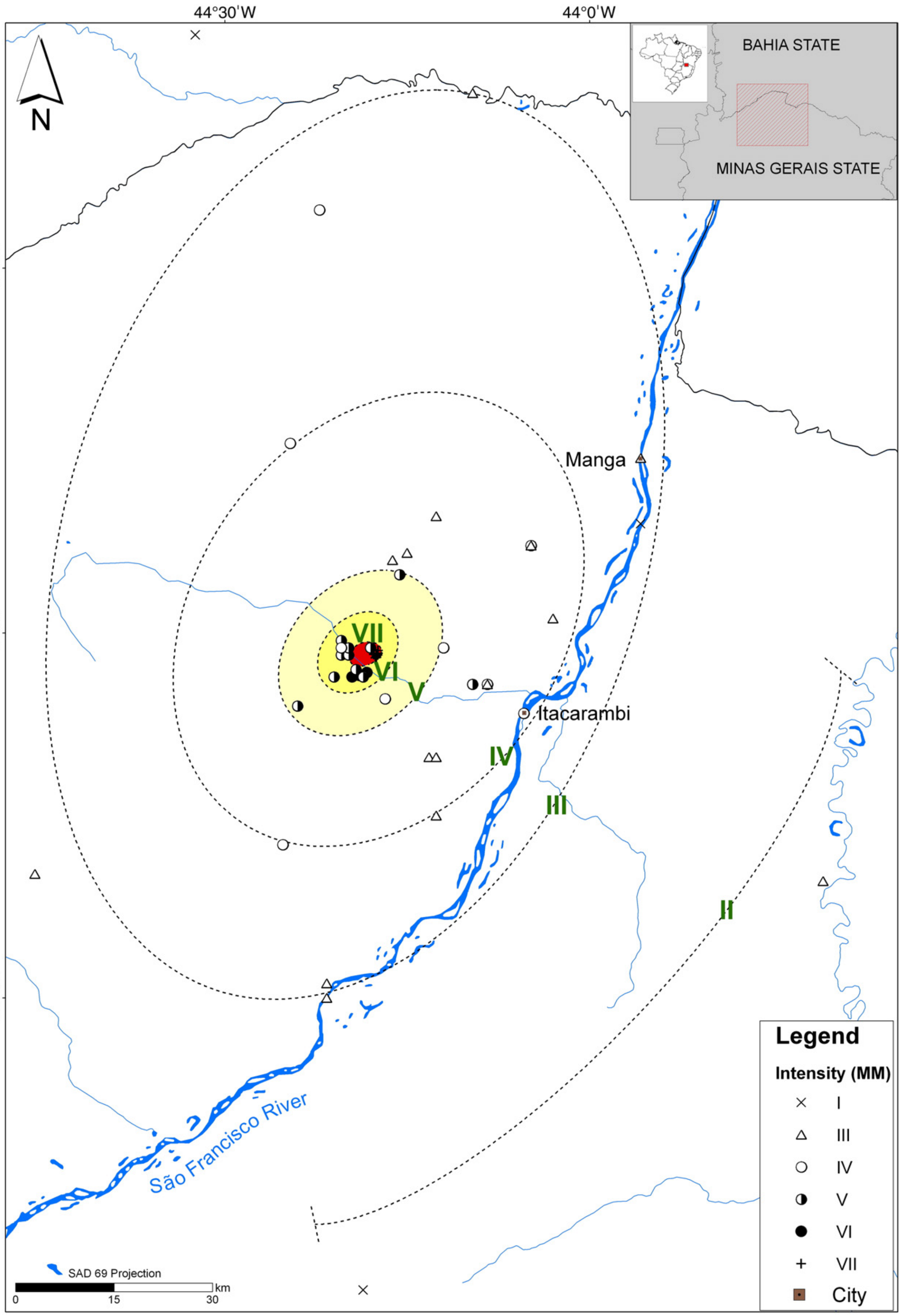

Fig. 2. Map with the isoseismal curves (dashed lines) for the December 9, 2007 (4.9 m_b) earthquake with Modified Mercalli (MM) intensities. The symbols represent MM intensities according to the legend. The inset map indicates the location of the study area (red hachured square) next to the border between the states of Minas Gerais and Bahia.

Table 1
Source parameters for the December 9, 2007 earthquake.

Origin time hh:mm:ss.ss	Latitude (°)	Longitude (°)	ERH (km)	Depth (km)	Magnitude/no. stations	RMS (s)	Reference
02:03:27.96	−15.0632	−44.3242	7.5	0.0f	4.5 m_b/23	0.98	IDC
02:03:29.44	−15.0480	−44.2310	16	10f	4.9 m_b/32	0.92	NEIC/USGS
02:03:28.36	−15.0326	−44.2953	0.2	0.65	4.3 m_R/6	0.02	This work

ERH — horizontal error.
f — fixed depth.

3.2. Local seismographic network

After the May 24, 2007, 3.5 magnitude event, the local seismic activity in the area continued to be felt in the following months, and motivated the deployment in October 23, 2007 of a 6-station network. The seismic stations were composed of broadband sensors CMG 6TD (Güralp Systems) with flat response from 30 s to 100 Hz, acquiring data continuously at a sampling rate of 400 Hz. During the period of seismic monitoring, the network configuration was changed. The first distribution of stations (October 23 to November 1) followed the estimated epicentral area of the 3.5 m_R event of May 24, determined with regional stations. After the epicentral determination of the first events detected by the local network, the distribution of stations was changed (November 1) to better constrain the hypocenters. Fig. 3 shows these two network configurations. The local network was deactivated in May 25, 2008, and only Station 7 remained to monitor the seismic activity.

3.3. Temporal distribution of the Caraíbas seismicity

Fig. 4 shows the temporal distribution of the seismicity detected by the local network (October 23, 2007 to May 25, 2008) and by the single Station 7 (May 26 to August 09, 2008). The figure includes all events with a threshold magnitude of about 0.5 m_D, comprising a total of 662 events. Large aftershocks occurred on March 19, 2008 and April 09, 2008, with magnitudes of 3.8 m_R and 3.1 m_D, respectively.

For the events detected only by the local network, we calculated duration magnitudes (m_D) using the coda duration in seconds (D), measured from the P-wave onset until the amplitude reaches the local noise level. The equations used (Assumpção et al., 1989) are:

$$m_D = 1.00 \log D - 0.02 \ (D \text{ less than } 30 \text{ s})$$
$$m_D = 2.05 \log D - 1.61 \ (D \ 30 \text{ or more}).$$

Because of operational problems, several data gaps occurred during the monitoring period, such as just after the peak of seismicity following the mainshock, from December 13 to 16, 2007, and the longest period of no data, starting in December 29, 2007, and lasting until January 31, 2008.

Despite the data gaps, a clear decrease in seismicity rate can be observed. An average of 2.5 events/day was detected until November 16, 2007. From November 17 to December 7, 2007, only three events were detected. Immediately before the mainshock, three events occurred on December 8, 2007. This pattern characterizes a 21-day seismic quiescence, followed by immediate precursors to the mainshock. The 21-day seismic quiescence for a magnitude 4.9m_b to 4.4 m_R is consistent with the empirical relations obtained from several other cases as compiled by Scholz (1990).

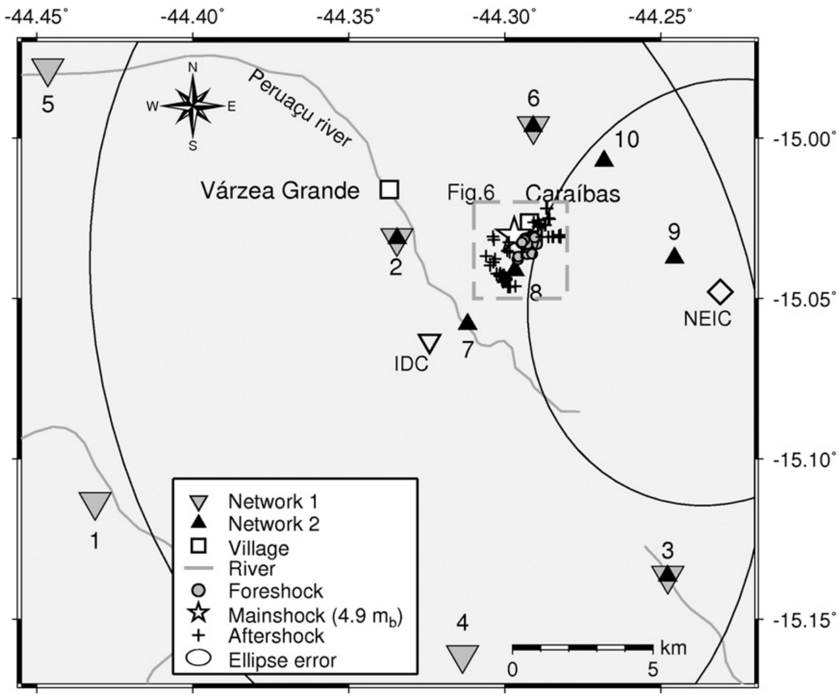

Fig. 3. Epicentral distribution of Caraíbas–Itacarambi seismicity. Gray inverse triangles and black triangles indicate the seismographic stations of the first and seconds networks, respectively (from JAN1 to JAN10). The gray circles, open star and crosses represent the foreshocks, mainshock and aftershocks, respectively. The open diamond and the open inverse triangle indicate the epicentral determination of the mainshock by NEIC and IDC agencies, respectively, with the error ellipses. White squares are villages.

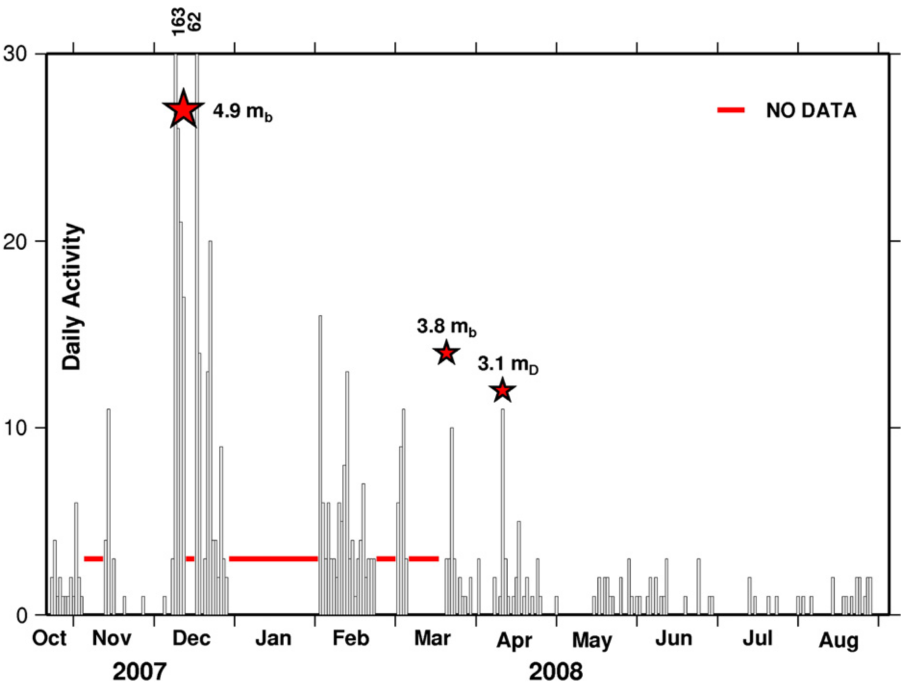

Fig. 4. Temporal distribution of the seismicity at Caraíbas-Itacarambi area from October 23, 2007 to August 9, 2008. Vertical bars indicate the daily number of events recorded by the local networks, the horizontal bars represent periods with no data from the local networks. The stars indicate the three largest events with their magnitudes. Notice the evidence of a seismic quiescence from mid November to early December 2007. The total numbers of events detected on December 9 and December 17, 2007, are indicated at the top of the histogram (163 and 62 events, respectively).

3.4. Hypocentral determination

From a total of 662 detected events we selected 95 with at least four P- and/or S-wave readings to perform the hypocentral determination using HYPO71 code (Lee and Lahr, 1975). An initial velocity model for the area was estimated based on geological data from wells drilled in sedimentary cover down to the crystalline basement (Nobre-Lopes, 2002; Martínez, 2007), geophysical studies of magnetic and gravimetric fields (da Cunha Filho, 2004), and information of water wells drilled in the north part of the Minas Gerais State (de Souza, 1995). In the Caraíbas–Itacarambi seismic area the thickness of the limestone layer varies between 50 and 200 m (Martínez, 2007). The initial model consists of two horizontal layers over a half-space. The most superficial layer has P-wave velocity of 3.5 km/s and thickness of 50 m, representing the limestones from the Sete Lagoas Formation. The second layer consists of 95 m of fractured gneiss from the Januaria Complex (basement of the São Francisco Craton), with P-wave velocity of 5.6 km/s. The half-space, comprising compact gneiss from the Januaria Complex, has P-wave velocity of 6.0 km/s. The Vp/Vs ratio of 1.720 ($\pm$0.003) was obtained by a composite Wadati diagram (Fig. 5). From the located events we selected a data set of 75 events (including the mainshock) with clear P- and S-wave arrivals, maximum RMS residual of 0.05 s, and magnitude above 1.0 m_D. These events have epicentral distances between 3.5 and 18 km (first network configuration) and 0.5 to 13 km (second one).

We also searched for a velocity model that gives the least overall RMS travel time residual for the 75 events, using genetic algorithm (Lopes et al., 2003), starting with the initial velocity model. P-wave velocities (Vp) and thicknesses at the two layers and the half-space were varied to find the model with the least overall RMS travel time residual in the hypocenter determinations. The best model has, from top to bottom, a first layer 0.1 km thick with Vp = 4.4 km/s; a second layer 0.5 km thick with 5.5 km/s and the half-space with Vp = 5.8 km/s.

After the determination of the hypocentral locations for all 75 events using this final velocity model obtained by the genetic algorithm, we applied the double-difference algorithm of Waldhauser and Ellsworth (2000) using the hypoDD code (Waldhauser, 2001) to relocate the events. This algorithm requires that the distance between two events is small compared to the distance of the pair to a single station. The double-difference algorithm attempts to minimize the difference between the travel time residuals (double-differences) for a pair of earthquakes at a single station, compensating for unmodeled velocity heterogeneities along the path.

The result of hypocentral determinations using hypoDD is shown in Fig. 6. The epicentral map for the 75 relocated events is shown in Fig. 6a. Fig. 6b shows the vertical profile along the continuous line AB

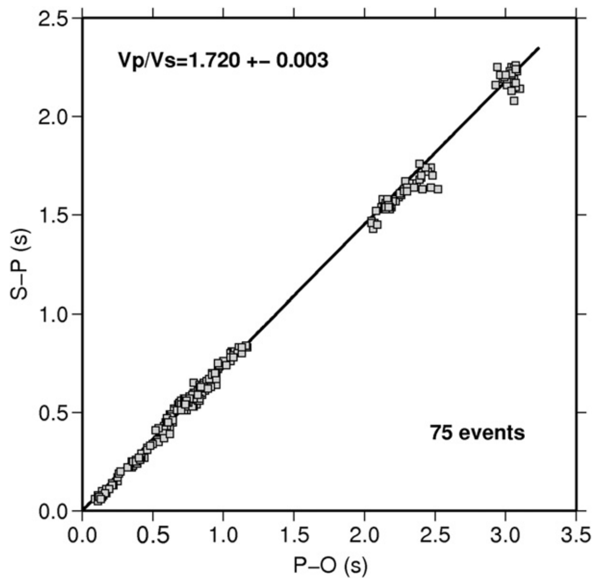

Fig. 5. Composite Wadati diagram for Caraíbas–Itacarambi seismicity determined using 75 events and 352 data (squares). The best fit (solid line) corresponds to a Vp/Vs ratio of 1.720 ($\pm$0.003).

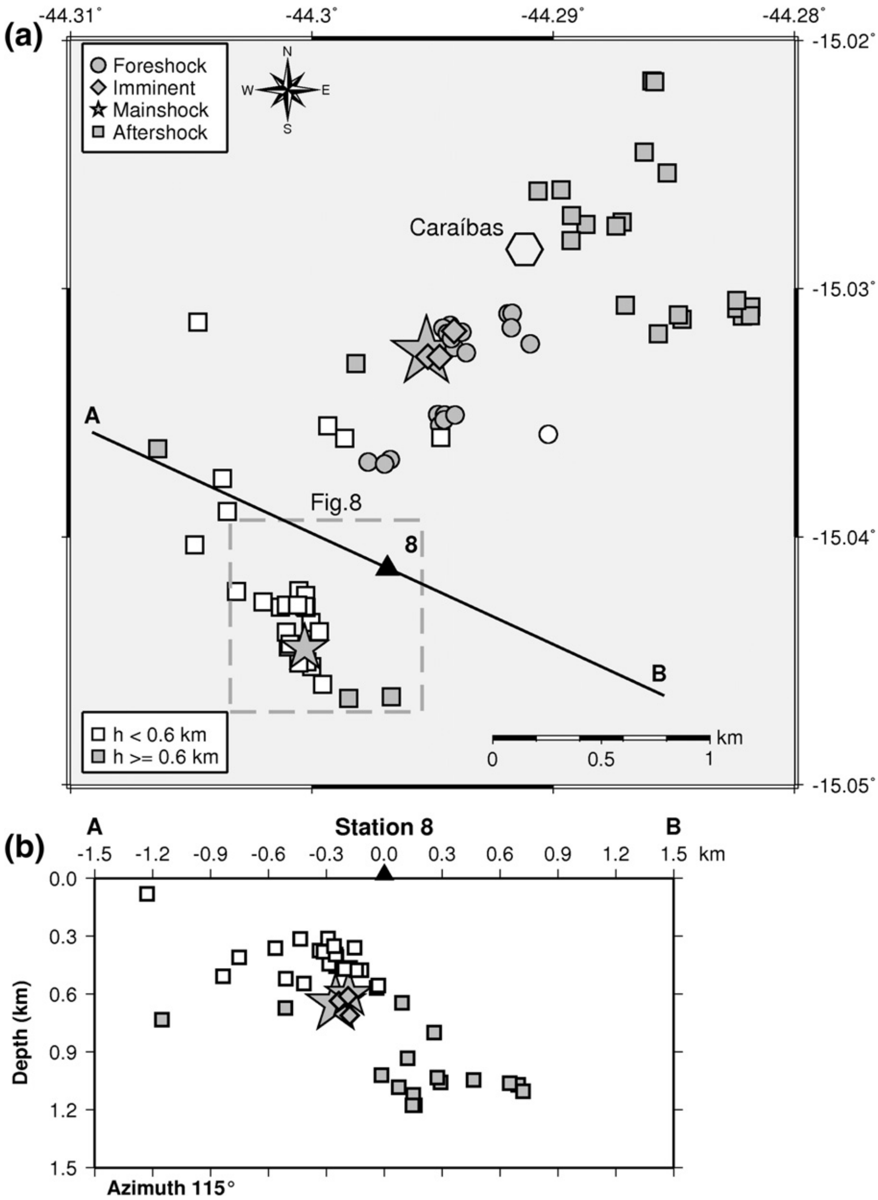

Fig. 6. (a) Map of the Caraíbas–Itacarambi seismicity showing foreshocks (circles), imminent foreshocks (diamonds), mainshock (large star) and aftershocks (squares). The little star corresponds to the 3.8 m_R magnitude aftershock. Events shallower than 0.6 km are shown in open symbols, and deeper in gray. Line AB indicates the direction (azimuth of 115°) of the vertical profile that passes through Station 8 (black triangle). The dashed box corresponds to the zoom area of Fig. 8. (b) Vertical section AB passing through Station 8 (black triangle) showing the depth distribution of the hypocenters. The symbols follow the pattern of Fig. 8a. Only events recorded by Station 8, with better constrained depths, are shown. The abscissa axis indicates relative distances in kilometers over the line AB, with positive values from Station 8 to point B and negative ones to A.

(azimuth of 115°) shown in the map passing through Station 8 (black triangle). The events are differentiated as foreshocks (circles), imminent foreshocks (diamonds), mainshock of December 9, 2007 (large star) and aftershocks (squares). The little star corresponds to the largest aftershock of March 19, 2008 (3.8 m_R). Depths shallower than 0.6 km are denoted by open symbols deeper by gray symbols.

The epicentral distribution suggests an approximately 3-km long zone roughly aligned in the NE–SW direction. Station 8 (second deployment) nearest to the epicenters better constrains the depths of the events. Only the events detected by this station (imminent foreshocks, the mainshock and most of the aftershocks including the largest one) have more reliable focus depths and are displayed in the vertical profile AB (Fig. 6b). The early foreshocks detected only by the first network stations, at larger distances from the epicenters and less constrained hypocentral depths, are not plotted in the profile. A general trend is seen with shallower events to the Northwest (depths between 0.3 and 0.6 km) and deeper to the Southeast (down to 1.2 km).

The fifteen events with epicenters near Station 8 (dashed box in Fig. 6a) were analyzed with more detail. We performed a visual P and S-waveform cross-correlation for the events of this cluster, as shown in Fig. 7, to get more accurate relative arrival times. The relocated hypocenters for this cluster are presented in Fig. 8, following the same symbol and color criteria used in Fig. 6. The continuous line AB, with azimuth of 115° (passing through Station 8) in Fig. 8a, defines the vertical profile presented in Fig. 8b. This vertical section shows that the events are well aligned starting with a depth of 0.4 km at the NW and reaching down to depths of approximately 0.8 km to the SE. This feature can be interpreted as the fault plane dipping to the SE with an angle of approximately 40°.

3.5. Focal mechanism

From the data set of 75 relocated events we used 37 events to determine composite focal mechanism using FPFIT code (Reasenberg

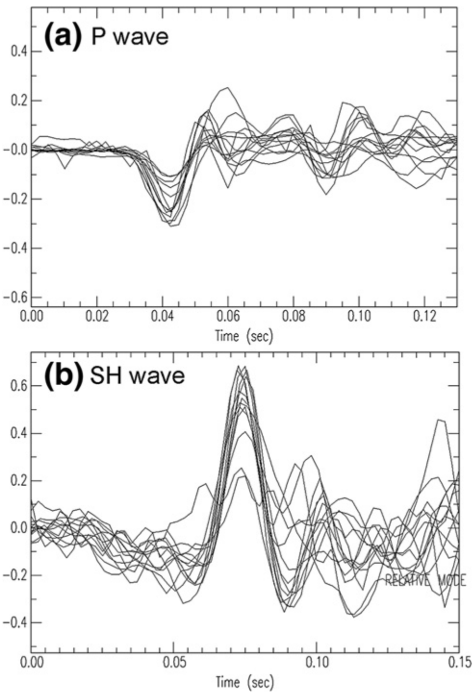

Fig. 7. Waveform correlations at Station 9 for the events located inside the dashed box of Fig. 6, using the vertical component for the P-wave (a) and N–S component for the S-waves (b).

and Oppenheimer, 1985), assuming that all the events have the same source mechanism. The selected 37 events have at least 8 readings (4 P- and 4 S-wave readings), azimuth gaps between 119° and 165°, RMS travel time residuals equal or lower than 0.035, and ERH (horizontal error) smaller than 0.20 km. A total number of 150 P-wave polarities from the data set of these 37 events were used to determine the composite focal mechanism. For some events the first polarities were affected by a-causal effects of the anti-alias digital filter, mainly at Station 7, which is the only station located in an outcrop. In these cases a correction was applied before reading the P-wave polarities.

For the local data set, the best FPFIT solution corresponds to a plane with strike 10°, dip of 70° and rake of 60° (Fig. 9a) Including P-wave polarities of regional and teleseismic stations (larger symbols in Fig. 9b) to the local data set, and using the hypocenter trends seen in Figs. 6 and 8, a preferred solution is given as 30° of strike, 40° of dip and 105° of rake (Fig. 9b). This is the adopted focal mechanism solution for the Caraíbas–Itacarambi seismicity. Some inconsistencies found for this solution (such as the compressional polarities of the local data in the SW quadrant) can be related to hypocentral errors causing large deviations in azimuth and take-off angles at Station 8. This fault plane solution corresponds to a reverse fault with near horizontal, E–W trending P-axis.

This result is similar to the focal mechanism solution obtained for another seismic activity that occurred near Manga, 50 km to the North of Caraíbas, occurred in 1990, which also showed a reverse mechanism with N–S trending fault (Assumpção et al., 1990) as shown in Fig. 1.

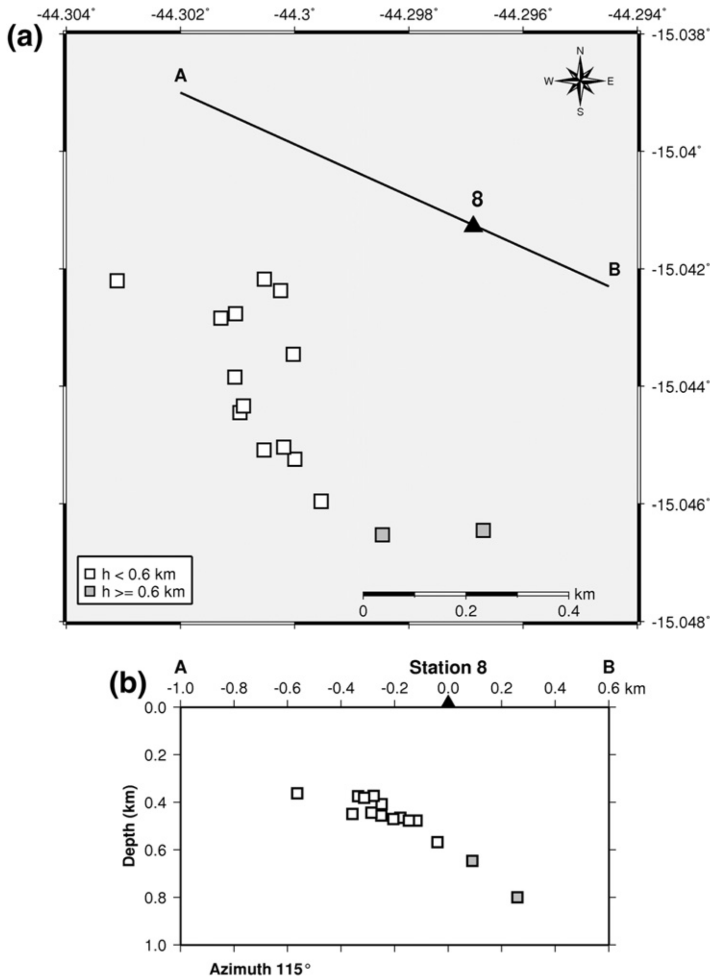

Fig. 8. (a) Map of the southern cluster (dashed box in Fig. 6). All the symbols and colors follow the pattern of Fig. 6; (b) vertical projection along line AB showing depth distribution of hypocenters indicating a dip of about 40° to the SE.

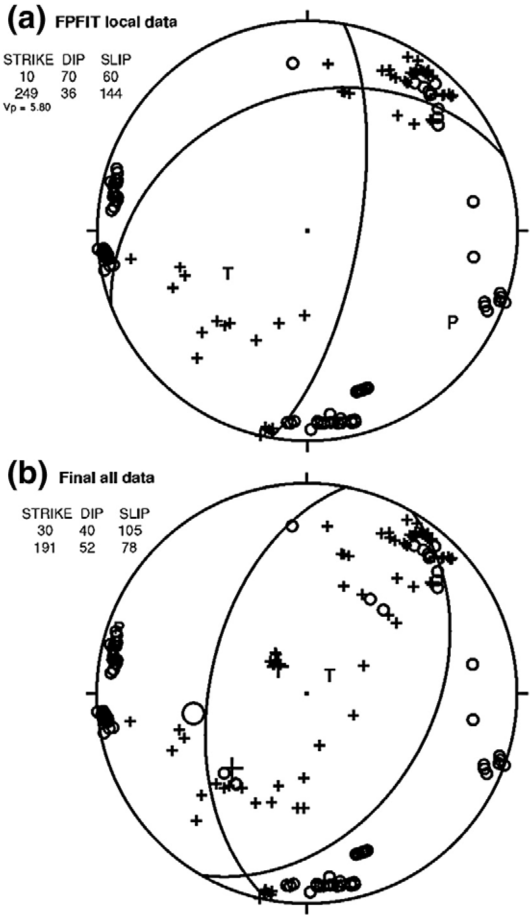

Fig. 9. Composite focal mechanism for Caraíbas–Itacarambi seismicity. (a) Result of FPFIT code using only local data. (b) Adopted final solution taking into account the local (small symbols), regional and teleseismic (larger symbols) polarities, as well as the hypocentral distribution. Circles and crosses represent dilatational and compressional P-wave first arrivals, respectively. P and T indicate the tension and compression axes, respectively.

Table 2
Focal mechanism solutions used to determine the stress tensor in the central part of the São Francisco Craton.

#	Location	Latitude (°)	Longitude (°)	Depth (km)	Strike (°)	Dip (°)	Rake (°)
1	Correntina/BA	−13.458	−44.554	0.6	342	71	68
2	Brasília/DF	−16.062	−47.599	2.2	280	70	70
3	Manga/MG	−14.575	−44.118	0.8	350	65	70
4	Encruzilhada/MG	−15.910	−40.910	1.0	335	25	90
5	Caraíbas–Itacarambi/MG	−15.0326	−44.2953	0.65	030	40	105

— event number.
Source: (1) and (2) — Lopes (2008); (3) — Assumpção et al. (1990); (4) — Veloso (1990); (5) — this work.

4. Discussion

The length of the rupture zone of the mainshock, as determined by the aftershocks, is about 3 km long. This is consistent with scaling relations for mid-plate earthquakes, which indicate a m_b magnitude between 4.5 and 5.0 for a 3 km rupture (Nuttli, 1983).

The shallow depth of the rupture is well constrained by the local network. Different velocity models, as discussed earlier, were used to locate the hypocenters and the best constrained focal depths are consistently less than about 1 km. Despite the shallow depth of the mainshock (less than 1 km), no clear topographical or geomorphological feature could be associated with the SSW–NNE fault plane. To investigate basement structural features, hidden beneath the limestone layers, we processed aeromagnetic data from a regional survey.

The data comprised 625 linear kilometers long profiles with direction N30°W, spaced 250 m apart, covering an area of 140 km^2 in the north of Minas Gerais State (SEME, 2000). We applied a first order vertical derivative to the anomalous magnetic field data for the study area. The vertical derivative is commonly used to enhance the shallowest geological sources, mainly structural lineaments. In the resulting image (Fig. 10), we can see NE–SW lineaments near the epicentral area, roughly parallel to the fault plane. These magnetic lineaments are probably related to basement fractures and faults.

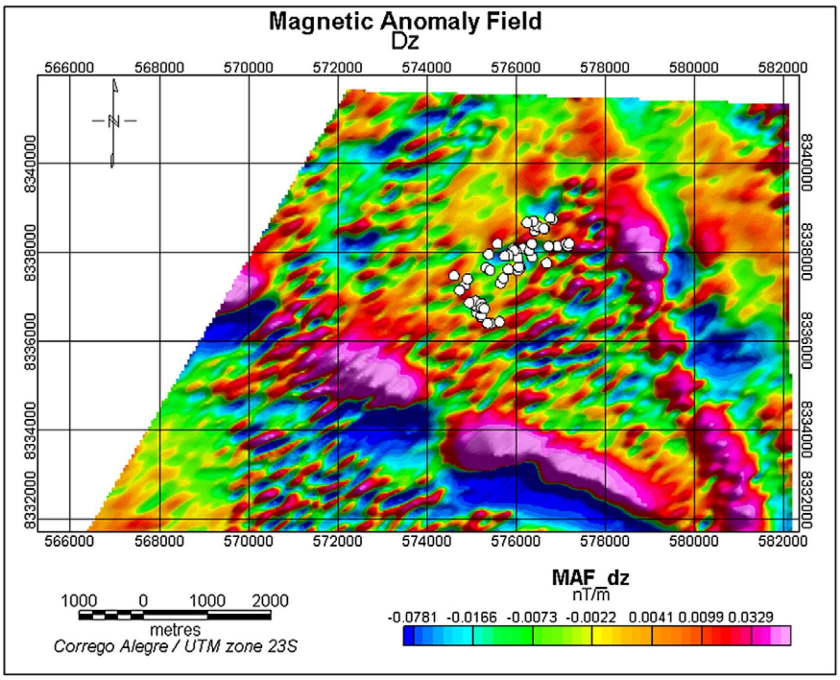

Fig. 10. First order vertical derivatives of the aeromagnetic field in the region of study. The white circles are the epicenters. Note the short-wavelength lineaments trending SW–NE near the epicentral area parallel to the fault strike.

Focal mechanisms of other events in the São Francisco Craton, two to the north of Caraíbas (Lopes, 2008; Assumpção et al., 1990), one to the east (Veloso, 1990), and one to the west (Lopes, 2008) are also reverse fault. Table 2 presents the focal mechanism solutions for these earthquakes. Stress inversion of these four events together with the Caraíbas–Itacarambi focal mechanism indicates an E–W compressional stress field (Lopes, 2008). Basement fractures and faults, oriented in the NE–SW direction, probably are being reactivated under the present E–W compressional stress field.

5. Conclusions

Detailed analysis of the hypocentral distribution of the Caraíbas–Itacarambi seismicity and P-wave polarity data observed at local, regional and teleseismic distances, indicates that the earthquakes occurred along one main fault rupture of about 3 km long by 2 km wide striking N30°E and dipping 40° to the Southeast. The focal depths range from approximately 0.3 to 1.2 km.

The seismicity at Caraíbas is probably a result of the reactivation of preexisting faults in the São Francisco Craton basement, with directions NE–SW and NNE–SSW, in response to the present E–W compressional stress field.

Acknowledgements

We thank the staff of Peruaçu Caves National Park, especially Ivan Borba Lima and Evandro Pereira da Silva, for logistic support during the field campaigns and the stations operations. We also thank Sidinei S. Tomás for the cooperation during installation and maintenance of the field equipments and Kate T. de Souza for the support in the generation of the macroseismic map. The authors thank Tectonophysics Editor Tom Parsons, and two anonymous reviewers for their comments and suggestions, which greatly improved our work.

References

Assumpção, M., 1983. A regional magnitude scale for Brazil. Bull. Seismol. Soc. Am. 73 (1), 237–246.

Assumpção, M., 1998. Seismicity and stresses in the Brazilian passive margin. Bull. Seismol. Soc. Am. 78 (1), 160–169.

Assumpção, M., Takeya, M., Ferreira, J.M., Costa, A., Sophia, C.M., 1989. Magnitude calculation and frequency–magnitude relation for João Câmara events, RN. Brazilian Geophysical Journal 7 (2), 107–116.

Assumpção, M., Veloso, J.A.V., Barbosa, J.R., Blum, M.L.B., Carvalho, J.M., Neves, E., Bassini, A., 1990. The Manga earthquakes, MG, March of 1990. XXXVI Brazilian Congress of Geology, 1990, Natal-RN. Proceedings of the XXXVI Brazilian Congress of Geology, vol. 6. SBG, Natal-RN, pp. 2154–2159.

Assumpção, M., Schimmel, M., Escalante, C., Barbosa, J.R., Rocha, M., Barros, L.V., 2004. Intraplate seismicity in SE Brazil: stress concentration in lithospheric thin spot. Geophys. J. Int. 159, 390–399.

Barros, L.V., Assumpção, M., Quintero, R., Caixeta, D., 2009. The intraplate Porto dos Gaúchos seismic zone in the Amazon craton — Brazil. Tectonophysics. doi:10.1016/j.tecto.2009.01.006.

Berrocal, J., Assumpção, M., Antezana, R., Dias Neto, C., Ortega, R., França, H., Veloso, J.A., 1984. Sismicidade do Brasil. Published by IAG/USP and Comissão Nacional de Energia Nuclear, Brazil, 320 pp.

CECAV, 2007. Base de dados geoespacializados de cavidades naturais subterrâneas do Centro Nacional de Estudo. Proteção e Manejo de Cavernas — CECAV. IBAMA.

Cordani, U.G., Sato, K., Teixeira, W., Tassinari, C., Basel, M.A., 2000. Crustal evolution of the South America Platform. In: Cordani, U.G., Thomaz filho, A., Milani, J. (Eds.), Tectonic Evolution of South America. CPRM, Rio de Janeiro, pp. 41–95. Org.

CPRM, 2003. Digital atlas of geology and mineral resources of Minas Gerais State, scale 1:500.000.

Cunha Filho, E.M. da, 2004. Contribution to the geology and evaluation of mineral potential in the Januária–Itacarambi–Montalvânia region (Minas Gerais State), Master Degree Thesis (in Portuguese), Institute of Geosciences, University of Brasília, 141 pp.

de Souza, S.M.T., 1995. Subsurface Water Availabilities of Minas Gerais State (in Portuguese).COPASA-MG. 525 pp.

Ferreira, J.M., Oliveira, R.T., Takeya, M.K., Assumpção, M., 1998. Superposition of local and regional stresses in northeast Brazil: evidence from focal mechanisms around the Potiguar marginal basin. Geophys. J. Int. 134, 341–355.

Johnston, A.C., 1989. Seismicity of stable continental interiors. In: Gregersen, S., Basham, P.W. (Eds.), Earthquakes at North-Atlantic Passive Margin: Neotectonics and Postglacial Rebound. Kluwer Acad, Norwell, Mass, pp. 299–327.

Johnston, A.C., 1996. Seismic moment assessment of earthquakes in stable continental regions.1. Instrumental seismicity. Geophys. J. Int. 124, 381–414.

Johnston, A.C., Kanter, L.R., 1990. Earthquakes in stable continental crust. Sci. Am. 262, 68–75.

Kenner, S.J., Segal, P., 2000. A mechanical model for intraplate earthquakes: application to the New Madrid seismic zone. Science 289 (5488), 2329–2332.

Lee, W.H.K., Lahr, J.C., 1975. HYPO71: a computer program for determining hypocenter, magnitude, and first motion pattern of local earthquakes. U.S. Geol. Surv. Open-File Rep, pp. 75–311.

Lopes, A.E.V., 2008. Focal Mechanisms and Lithospheric Stresses in Brazil. PhD Thesis (in Portuguese), IAG, University of São Paulo, 300 pp.

Lopes, A.E.V., Assumpção, M., Barbosa, J.R., 2003. Modelagem da Estrutura Crustal Média em Goiás com Algoritmo Genético. 8th International Congress of the Brazilian Geophysical Society, Rio de Janeiro. CD-ROM.

Martínez, M.I., 2007. Stratigraphy of Bambuí Group at the north of the São Francisco River Valley, MG. Master Degree Thesis (in Portuguese), Institute of Geosciences, Federal University of Minas Gerais, 122 pp.

Nobre-Lopes, J., 2002. Diagenesis of the dolomites hosting Zn/Ag mineral deposits in the Bambui Group at Januaria Region-MG, PhD Thesis, University of Campinas, Campinas, São Paulo, Brazil, 183 pp.

Nuttli, O., 1983. Average seismic source-parameter relations for mid-plate earthquakes. Bull. Seismol. Soc. Am. 73 (2), 519–535.

Reasenberg, P., Oppenheimer, D., 1985. FPFIT, FPPLOT and FPPAGE: Fortran computer programs for calculating and displaying earthquake fault-plane solutions. U.S. Geol. Surv. Open-File Rep. 85-739. 109 pp.

Scholz, C.H., 1990. The Mechanics of Earthquakes and Faulting. Cambridge U.P. 439 pp.

Schulte, S.M., Mooney, W.D., 2005. An updated global earthquake catalogue for stable continental regions: reassessing the correlation with ancient rifts. Geophys. J. Int. 161, 707–721.

SEME, 2000. Aerogeophysical Survey in the North of Minas Gerais State. Area 5. Secretaria Estadual de Minas e Energia (SEME), Minas Gerais, Brazil. in Portuguese.

Sykes, L.R., 1978. Intraplate seismicity, reactivation of preexisting zone of weakness, alkaline magmatism, and other tectonism posdating continental fragmentation. Rev. Geophys. Space Phys. 245, 298–302.

Talwani, P., 1989. Characteristic features of intraplate earthquakes and the models proposed to explain them. In: Gregersen, S., Basham, P.W. (Eds.), Earthquakes at North Atlantic Passive Margins: Neotectonics and Post-Glacial Rebound. Kluwer, Dordrecht, pp. 289–297.

Talwani, P., Rajendran, K., 1991. Some seismological and geometric features of intraplate earthquakes. Tectonophysics 186, 19–41.

Tassinari, C.C.G., Bettencourt, J.S., Geraldes, M.C., Macambira, M., Lafon, J.M., 2000. The Amazonian Craton. In: Milani, J., Thomaz filho, A. (Eds.), Tectonic Evolution of South America. CPRM, Rio de Janeiro, pp. 41–95. Org.

Veloso, J.A.V., 1990. Atividade sísmica de Encruzilhada-BA. 36th Brazilian Congresso of Geology, Natal. in Portuguese.

Waldhauser, F., 2001. HYPODD — a program to compute double-difference hypocenter locations. U.S. Geol. Surv. Open-File Rep, pp. 01–113.

Waldhauser, F., Ellsworth, W.L., 2000. A double-difference earthquake location algorithm: method and application to the Hayward fault. Bull. Seismol. Soc. Am. 90, 1353–1368.